WARSAW UNIVERSITY OF TECHNOLOGY Index 351733
FACULTY OF CIVIL ENGINEERING
COMMITTEE FOR CIVIL AND WATER ENGINEERING
POLISH ACADEMY OF SCIENCES ISSN 1230-2945

DOI: 10.24425/ace.2025.155109

ARCHIVES OF CIVIL ENGINEERING

Vol. LXXI ISSUE 3 2025

pp. 431 –445

Research paper

Corrosion models of a mounded horizontal pressure vessel in a probabilistic approach

Mateusz Sondej[1], Przemysław Sorn[2], Jarosław Górski[3]

Abstract: The computations of fuel tanks are bound to cover uncertainties related to geometric and material imperfections, post-welding stresses, non-uniform settlement, and shell degradation due to corrosion. The paper compares four different methods of tank corrosion descriptions: a uniform reduction of the sheet thickness of the entire shell, degradation described by an angle correlated with its partial fuel filling, corrosion patterns defined by appropriately selected trigonometric functions, and an advanced model using theoretical random fields. All corrosion patterns were numerically investigated to identify their impact on structural response. The computations were carried out for a simplified numerical model of a mounded horizontal pressure vessel. The Point Estimate Method (PEM) was used to estimate the mean value and standard deviation of the shell critical forces. The probabilistic approach allows to assess structural reliability and makes it possible to optimize the structure. It has been shown that the optimal variant of corrosion description, easy for engineering applications, is the uniform reduction of the shell thickness.

Keywords: mounded fuel tanks, shell corrosion models, limit states, probabilistic description

[1]PhD., Eng., Gdańsk University of Technology, Faculty of Civil and Environmental Engineering, 11/12 Gabriela Narutowicza Street, 80-233 Gdansk, Poland, e-mail: matsonde@pg.edu.pl, ORCID: 0000-0002-3574-7089
[2]MSc., Eng., Gdańsk University of Technology, Faculty of Civil and Environmental Engineering, 11/12 Gabriela Narutowicza Street, 80-233 Gdansk, Poland, e-mail: s120645@o365.student.pg.edu.pl, ORCID: 0000-0003-1299-1940
[3]Prof., DSc., PhD., Eng., Gdansk University of Technology, Faculty of Civil and Environmental Engineering, 11/12 Gabriela Narutowicza Street, 80-233 Gdansk, Poland, e-mail: jaroslaw.gorski@pg.edu.pl, ORCID: 0000-0002-6478-0216

1. Introduction

Pressure vessels are essential structures to store fuel and other petroleum industry products. The tank damage may cause substantial economic and environmental aftermath and threat to human life and health. Therefore, it is substantial to provide relevant reliability and durability of this structural category, among others included in the PED directive [1]. The standard guidelines require reliability analysis only in the CC3 consequence class case [2]. The numerical measure of reliability level is the reliability index β, its values are included in [2]. After 50 years of tank use its reliability index β is required not to fall under the level of 4.3. However, the standards never specify the methods to numerically assess the reliability. It is assumed that the use of the standard safety factors assures the required structural safety. The alternative standards allow for direct reliability assessment in design [3]. Thus the optimal solutions should be investigated and shown, directed to specific engineering structures, e.g. pressure vessels, whose design and manufacture are unified to a great extent.

Reliability estimation is bound to cover all the aspects linked with design, fabrication, and operation of tanks. The advanced computations, fundamental in structural design, are bound to consider geometric and material imperfections [4], post-welding stresses [5], non-uniform settlement [6], and the cyclic pattern of tank filling [7] or seismic loading [8]. An issue that is challenging and difficult to control is corrosion of the tank sheets [9, 10]. Corrosion usually occurs in aged pressure vessels employed in industrial processes, caused by aggressive media inside or severe environmental conditions outside the tank. Standard rules and computational algorithms involving strength of corroded shells are based on uniform thickness reduction. Since the corroded surface is uneven, a much higher accuracy level is required. The work [11] compares the ultimate strength of corroded plates of uniform thickness and irregular surface.

The research on corrosion processes of tanks incorporates analytical solutions. The work [12] proposes a method to assess the critical time of stability loss in thin-walled high-pressure vessels subjected to uniform corrosion. In [13] a simplified method is developed for the Fitness-for-service (FFS) assessment of pressure vessels undergoing corrosion damage. In turn, the paper [14] addresses FFS assessment of spherical pressure vessels with localized corrosion. The paper [15] covers the effect of pitting corrosion on stress concentration factor (SCF) for a spherical pressure vessel. A series of finite element models are investigated, to prove that the pit aspect ratio is a principal stress-related parameter. The item [16] delivers strength and stability algorithm involving unknown thickness of a corroded vessel. The paper [17] shows a unified closed-form solution for the lifetime of elastic spherical and cylindrical vessels of arbitrary thickness, subjected to the pressure of corrosive media.

Corrosion processes are often analysed with the use of a probabilistic framework. The authors of [18] conduct a structural analysis to identify reliability index variation, produced by both general corrosion and pitting corrosion in the vessels. The in situ and laboratory tests are substantial while modelling tank corrosion and its results. The work [19] includes laboratory tests performed on pressure vessel plates. The Monte Carlo simulation points out that the population of mechanical properties of the corroded specimens follows the Gaussian variable type. The paper [20] collects the thickness profile data for backside corrosion of the bottom floors of several oil storage tanks, the data are statistically processed to investigate the corrosion

risk of the bottom floors. The slope of the risk is a relevant evaluation parameter involving discrete thickness data. In the work [21] various statistical characteristics of the generated random fields are investigated to identify their impact on structural response. Attempts are also made to estimate the reliability of corroded tanks (time-to-failure forecast) [22].

Numerical modelling of corrosion headed for design deserves attention. The analysis is not intended to show the most inconvenient corrosion patterns to cross the limit of buckling tank loads. It is rather bound to simulate real corrosion patterns on the tank shell. The major task of the work is to assume various probabilistic models of corrosion layout, and next, to estimate the mean value and standard deviation of the limit load. Four different corrosion models are compared. First, standard forms of overall uniform tank degradation are considered. Next, partial tank degradation is linked with its partial fuel filling. Moreover, simulations of corrosion zones are implemented by simplified trigonometric function models and the use of advanced theoretical random fields defined by correlation functions. This sort of analysis allows for structural reliability estimation and sensitivity assessment of the limit state variation due to corrosion process impact. It is essential to assume optimal background to estimate the reliability of a designed tank [23–25]. Such a computational algorithm may be called reliability optimization of pressure tanks.

In all cases, the Point Estimate Method (PEM) [26] was used in the probabilistic calculations. This avoids the serial, time-consuming calculations needed when using the Monte Carlo method, the Response Surface Method, and many others [27, 28]. An important element is the adoption of an optimal data description allowing for the estimation of the reliability of the designed tank. The main purpose of the work is to answer the question of whether the corrosion model defined by a uniform change in shell thickness is a sufficient description of tank degradation, replacing more complicated models.

The analysis of corrosion impact on structural resistance and reliability is illustrated by a mounded horizontal pressure vessel. The preliminary results of calculations of pressure vessels, taking into account material corrosion, are presented in [29].

2. The mounded vessel FEM model

The analysis concerns a mounded storage horizontal pressure vessel with a length of 72599 mm and a diameter of 5600 mm (Fig. 1). The cylindrical shell is 28 mm thick, while the hemispherical ends are 26 mm thick. The base material used for tank manufacture is steel P355NL2. The cylindrical shell is stiffened with 13 T-shaped rings. There are five manholes in the upper part of the vessel.

The computations were performed for a part of the cylindrical shell between two circumferential rings (Fig. 2). The shell was characterized by the following parameters: length $L = 4785$ mm, diameter $d_c = 5600$ mm, and model thickness $t = 24.7$ mm (Fig. 2). This numerical model is consistent with the calculations of the standard critical force of tanks [3]. The model thickness results from reducing the design thickness of 28 mm by the so-called corrosion additive, in this case, 3.3 mm [3]. Boundary conditions were applied to both circular shell edges. The radial and circumferential translations were fixed, which corresponds to

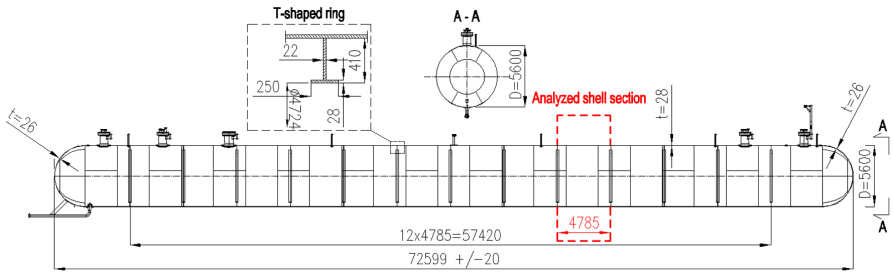

Fig. 1. The analysed mounded fuel storage vessel

simplified assumptions for heavy ring stiffeners. The shell was subjected to negative pressure and longitudinal compression [29]. The initial value of the negative pressure was assumed as $p = -1.0$ MPa. The calculations were carried out using the ABAQUS software [30]. The numerical model of the cylindrical shell consisted of shell elements S4R with reduced integration. The cylinder circumference was divided into 128 finite elements. The size of the rectangular shell elements was approximately 137×137 mm^2. The total number of shell elements was 4480. Linear buckling analysis (LBA) was performed. In all analyzed cases, the vessel's critical forces P_{cr} were determined.

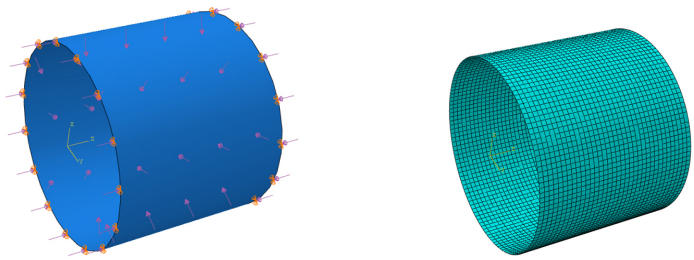

(a) (b)

Fig. 2. Simplified model of the tank part: (a) loads and boundary conditions; (b) mesh

3. The models of corroded shell of a pressure vessel

The FEM models decisive for the corrosion range of a tank shell material may be formed on various accuracy levels. Due to the random character of the phenomenon, it seems reasonable to launch the probabilistic mode. The simplest, straightforward model assumes uniform tank deterioration captured by a single random variable, i.e. shell thickness t. However, the actual measurements of tanks [19, 20] point out random characters of parameters and the layout of corroded zones. For this reason, more complicated models of the corroded tank can be used. In the case of cylindrical horizontal tanks, the corrosion impact can be defined by an angle α to show the cylinder section subjected to deterioration. The regular corrosion layout may be

also the result of trigonometric functions applied in computations. The improved corrosion map may be generated using random fields and properly adjusting correlation functions. The impact of these four variants of corrosion models on the critical force of the shell is assessed. On these bases, conclusions may be drawn from corrosion modelling in vessel structures.

3.1. Corrosion modelled by a single random variable

The first variant regards corrosion by a single variable, the tank thickness t. The thickness variation is uniform, displaying a constant value throughout the shell. This is the most straightforward way to capture uncertainties in numerical analysis.

A probabilistic attempt at corrosion description requires the assumption of a random shell thickness t model. Due to the shortage of comprehensive statistical data, the shell thickness t is considered a Gaussian variable $N(\bar{t}, \sigma_t)$ defined by its mean value $\bar{t}$ and standard deviation σ_t. Since the corrosion allowance of the vessel is 3.3 mm [3], i.e. approximately 12% of the nominal thickness of the sheet, the following average thickness of the corroded sheet was assumed $\bar{t} = 28 - 3.3 = 24.7$ mm. To limit the shell thickness t to values lower than 28 mm the standard deviation of 1/3 of the vessel corrosion allowance was stated, i.e. $\sigma_t = 3.3/3 = 1.1$ mm. Hence the generated sheet thickness ranges from $\bar{t} - 3\sigma_t = 21.4$ mm to $\bar{t} + 3\sigma_t = 28.0$ mm.The Gaussian variable allows for an infinitely large dispersion of t, however, the probability of exceeding the assumed interval is lower than 0.1%. Moreover, the generation of Gaussian variable t bigger than the nominal thickness is justified by fabrication tolerance. On the other hand, the maximum reduction of sheet thickness $t < 21.4$ mm, below 24% of the lowest thickness is also possible and reasonable. The measurement data show, that the bottom sheet thickness reduction of vertical cylindrical tanks ranges 10%÷40% [19]. Hence the generation of corrosion decrement does not yield limitations, e.g. bounded Gaussian or log-normal variables. Finally, the sheet thickness is considered a Gaussian variable $N_t(\bar{t}, \sigma_t) \equiv N_t(24.7, 1.1)$ [mm].

The probabilistic analysis employs the PEM (Point Estimate Method) [26], while it takes a low computational amount, and is easy to implement in engineering calculations. In the PEM a continuous random variable X of a distinct density function $f_X(x)$ is replaced by a discrete variable $p_X(x)$. Further simplifications are applicable in symmetric Gaussian variables (no skewness). While a single random variable is involved the probability density function may be represented by two discrete points – impulses. The first and second moments of the shell critical force, i.e. the mean value $\hat{P}_{\mathrm{cr}}$ and variance $\hat{\sigma}^2_{P_{\mathrm{cr}}}$ can be estimated [26]:

$$\begin{aligned} \hat{P}_{\mathrm{cr}} &= 0.5(P^-_{\mathrm{cr}}) + 0.5(P^+_{\mathrm{cr}}) \\ \hat{\sigma}^2_{P_{\mathrm{cr}}} &= 0.5(P^-_{\mathrm{cr}})^2 + 0.5(P^+_{\mathrm{cr}})^2 - (\hat{P}_{\mathrm{cr}})^2 \end{aligned} \tag{3.1}$$

The critical forces P^-_{cr} and P^+_{cr} calculations are conducted in the cases of two tank models, different in the t thickness of the shell:

$$\begin{aligned} t_- &= \bar{t} - \sigma_t = 24.7 - 1.1 = 23.6 \text{ mm} \quad \rightarrow P^-_{\mathrm{cr}} = -0.770 \text{ MPa} \\ t_+ &= \bar{t} + \sigma_t = 24.7 + 1.1 = 25.8 \text{ mm} \quad \rightarrow P^+_{\mathrm{cr}} = -0.973 \text{ MPa} \end{aligned} \tag{3.2}$$

The form of the deformed shell in the case of $t_- = 23.6$ mm is shown in Fig. 3.

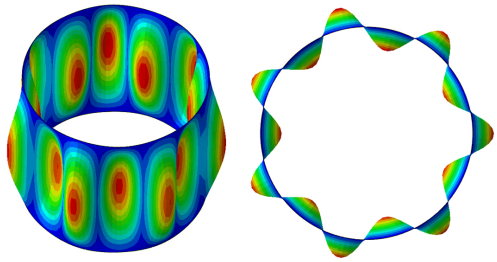

Fig. 3. The loss of the tank stability caused by the uniform model of the shell corrosion, $t_- = 23.6$ mm

Based on the computations the formulas (3.1) lead to the estimators of the critical force mean value $\hat{P}_{\rm cr} = -0.872$ MPa, and standard deviation $\hat{\sigma}_{P_{\rm cr}} = 0.097$ MPa. Additionally, the structural limit state $P_{\rm cr} = -0.867$ MPa is determined concerning the mean corrosion decrement $t = 24.7$ mm. This value differs from the value of $\hat{P}_{\rm cr}$ to a slight extent only.

3.2. Corrosion modelled by two random variables

The second computational variant assumes two random variables, i.e. thickness of the shell t, and the corroded zone defined by the angle α (Fig. 4). The thickness t is considered a Gaussian variable, following the first variant, i.e. $N_t(24.7, 1.1)$ [mm]. The angle α denoting a weakened cylindrical tank section may be linked with partial tank filling.

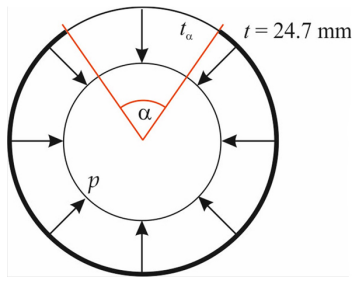

Fig. 4. Illustration of the assumed shell part of reduced sheet thickness

To formally take into account the scatter of the angle α the uniform random variable is assumed. While the angle α ranges the entire tank, i.e. the interval $0.0 \leqslant \alpha \leqslant 2\pi$, the mean value $\bar{\alpha}$ and standard deviation σ_a read:

$$\bar{\alpha} = \frac{0 + 2\pi}{2} = \pi, \quad \sigma_\alpha^2 = \frac{(2\pi - 0)^2}{12} = \frac{1}{3}\pi^2, \quad \sigma_a = 0.577\pi \tag{3.3}$$

In the case of two random variables the following PEM formulas are applied [26]:

$$\begin{aligned} \hat{P}_{\rm cr} &= 0.25(P_{\rm cr}^{++} + P_{\rm cr}^{+-} + P_{\rm cr}^{-+} + +P_{\rm cr}^{--}) \\ \hat{\sigma}_{P_{\rm cr}}^2 &= 0.25\left[(P_{\rm cr}^{++})^2 + (P_{\rm cr}^{+-})^2 + (P_{\rm cr}^{-+})^2 + (P_{\rm cr}^{--})^2\right]^2 - (\hat{P}_{\rm cr})^2 \end{aligned} \tag{3.4}$$

Calculations of critical forces were made for four variants of random variables α and t:

$$\begin{aligned} &t = \bar{t} + \sigma_t = 25.8 \text{ mm}, \quad \alpha = \bar{\alpha} + \sigma_\alpha = 1.577\pi \quad \rightarrow P_{\text{cr}}^{++} = 0.919 \text{ MPa} \\ &t = \bar{t} + \sigma_t = 25.8 \text{ mm}, \quad \alpha = \bar{\alpha} - \sigma_\alpha = 0.423\pi \quad \rightarrow P_{\text{cr}}^{+-} = 0.979 \text{ MPa} \\ &t = \bar{t} - \sigma_t = 23.6 \text{ mm}, \quad \alpha = \bar{\alpha} + \sigma_\alpha = 1.577\pi \quad \rightarrow P_{\text{cr}}^{-+} = 0.785 \text{ MPa} \\ &t = \bar{t} - \sigma_t = 23.6 \text{ mm}, \quad \alpha = \bar{\alpha} - \sigma_\alpha = 0.423\pi \quad \rightarrow P_{\text{cr}}^{--} = 0.832 \text{ MPa} \end{aligned} \tag{3.5}$$

On this basis, the first and second moments were determined according to (3.4): the expected value $\hat{P}_{\text{cr}} = -0.8536$ MPa and standard deviation $\hat{\sigma}_{P_{\text{cr}}} = 0.0502$ MPa. For comparison, the average value of the critical load calculated in a standard way ($t = 24.7$ mm, $\alpha = \pi$) is $P_{\text{cr}} = -0.89409$ MPa, so is greater than estimated by the PEM. The deformations of the tank models are presented in Fig. 5.

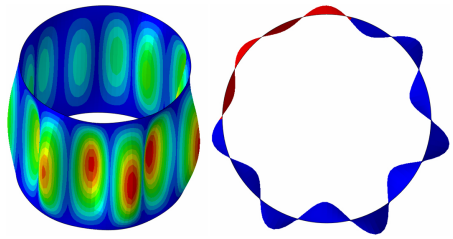

Fig. 5. Deformation of the tank model caused by the corrosion of a shell fragment ($\alpha = 0.423\pi$)

3.3. Corrosion modelled by a regular sine field

Corrosion measurements of real structures indicate that the distribution of material deterioration is not uniform. Moreover, the size and distribution of more heavily corroded areas are random. To simplify the data input describing the actual condition of the tank, corrosion fields were generated using the sine function. In this case, the random variables are the thickness of the shell t, and the number of waves in the horizontal and vertical directions, defined by integers n_x and n_y

$$t(x, y) = t \sin \varphi_x \sin \varphi_y = t \sin\left(n_x \frac{\pi}{l_x} x\right) \sin\left(n_y \frac{\pi}{l_y} y\right) \tag{3.6}$$

where: $l_x = 2\pi r = 2\pi 2800.0 = 17592.92$ mm is the length of the cylinder, and $l_y = 4785.00$ mm is the height of the shell part (Fig. 1).

To reduce the number of variables, a constant value of the number of half-waves along the height of the shell model was assumed, i.e. $n_x = 3$. The use of PEM requires the determination of the mean value and standard deviation of the random variables n_y. Assuming a maximum of 12 half-waves, the variable can take the following values (integers only) $n_y = 0, 1, \ldots, 12$, where 0 means a shell with uniform corrosion. According to a uniform distribution, the following approximate expected value and standard deviation of n_y can be determined (compare Eq. 3.3) $\overline{n}_y = 6$ and $\sigma_{n_y} = 3.46$. Finally, the following value was adopted $\sigma_{n_y} = 3$. The thickness t is described by a normal distribution $N_t(\bar{t}, \sigma_t) \equiv N_t(24.7, 1.1)$ mm and changes according to the sine function (3.6). Corrosion field for $n_x = n_y = 3$ is shown in Fig. 6a.

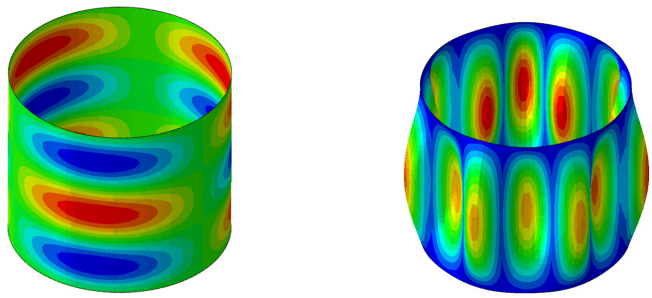

(a) (b)

Fig. 6. Corrosion fields described by function (3.6) for $n_x = n_y = 3$: (a) corroded field; (b) critical shell deformation

According to the PEM formulas, the critical load can be determined in four cases:

$$
\begin{aligned}
&t = \bar{t} + \sigma_t = 25.8 \text{ mm}, \quad n_x = 3, \quad n_y = \bar{n}_y - \sigma_{n_y} = 3 \rightarrow P_{\text{cr}}^{++} = 0.9704 \\
&t = \bar{t} + \sigma_t = 25.8 \text{ mm}, \quad n_x = 3, \quad n_y = \bar{n}_y + \sigma_{n_y} = 9 \rightarrow P_{\text{cr}}^{+-} = 0.9718 \\
&t = \bar{t} - \sigma_t = 23.6 \text{ mm}, \quad n_x = 3, \quad n_y = \bar{n}_y - \sigma_{n_y} = 3 \rightarrow P_{\text{cr}}^{-+} = 0.7673 \\
&t = \bar{t} - \sigma_t = 23.6 \text{ mm}, \quad n_x = 3, \quad n_y = \bar{n}_y + \sigma_{n_y} = 9 \rightarrow P_{\text{cr}}^{--} = 0.7682
\end{aligned} \tag{3.7}
$$

On the basis of the obtained results, the expected value $\hat{P}_{\text{cr}} = 0.8694$ MPa and standard deviation $\hat{\sigma}_{P_{\text{cr}}} = 0.1017$ MPa were estimated. The deformation of the tank model is presented in Fig. 6b.

3.4. Simulation of tank corrosion distribution using a random field

Geometric imperfections of tank shells or dispersion of material parameters, as well as two-dimensional models of corrosion degradation, can be described with appropriate random fields. Many computer programs have been developed to generate random theoretical fields focused on various issues. The most commonly used algorithms are based on Karhunen-Loëve expansion or using a wavelet-Galerkin approach [31]. An alternative original solution was adopted in the work. Corrosion field generations were performed using proprietary software described e.g. in [32]. The computational algorithm was used in the analysis of various issues, e.g. shell structures [33], imperfections of geometric silos [34], or composites [35].

The theoretical basis for generation of Gaussian random fields is an optimized version of the conditional acceptance and rejection method [32]. A conditional function $f(\mathbf{X}) = f(\mathbf{X}_u/\mathbf{X}_k)$ was introduced to the computational algorithm, enabling generation of the unknown part of the vector of random variables $\mathbf{X}_u$, assuming that the remaining elements of the vector $\mathbf{X}_k$ are known (previously generated) [32]

$$
f(\mathbf{X}_u/\mathbf{X}_k) = (\det \mathbf{K}_c)^{-1/2}(2\pi)^{-m/2} \exp(-0.5(\mathbf{X}_u - \overline{\mathbf{X}}_c)^T \mathbf{K}_c^{-1}(\mathbf{X}_u - \overline{\mathbf{X}}_c)), \tag{3.8}
$$

where $\mathbf{K}_c$ is a conditional covariance matrix, $\overline{\mathbf{X}}_c$ is the conditional mean value vector and m is the size of the matrix $\mathbf{K}$.

There are no restrictions imposed on the covariance functions defining the correlation matrix **K**. Thus, the algorithm allows the simulation of homogeneous or non-homogeneous fields, strongly or weakly correlated. It is also possible to introduce a correlation matrix obtained on the basis of measurements made in situ or using the results of laboratory tests.

The adopted propagation scheme $c \times d$ covering sequentially the generated field area (Fig. 7) plays an important role in the calculations. The generation process takes place in several stages. In subsequent steps, based on the previously generated points from the area, only one point value of the field is generated (Fig. 7). The propagation scheme $c \times d$ is successively moved to cover all points of the field.

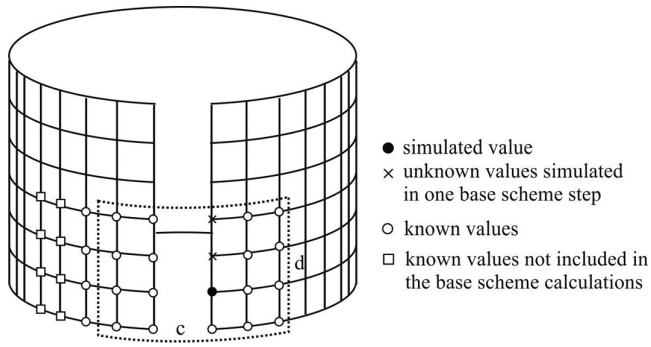

Fig. 7. Covering the generated area with the propagation scheme ($c \times d$) in the case of a cylinder

The original proprietary simulation method allows the generation of two-dimensional random fields described on cylinders. The algorithm enables closing the field to maintain the continuity of the description characterizing the cylinder surface. The propagation scheme $c \times d$ is therefore assigned to points located on both sides of the edges closing the cylinder (Fig. 7). The specific generation method is particularly important in the case of simulating geometrical imperfections of tanks [32].

In applying random fields, the most important element is the adoption of a correlation function appropriate for a given problem. In standard engineering problems, the exponential correlation function associated with the first-order autoregression function of the Markov process is most often used. In the two-dimensional case, it has the following form

$$t(x, y) = \exp\left(-d_x |x| - d_y |y|\right) \tag{3.9}$$

where d_x and d_y are the damping parameters describing the decay of the correlation, and $|x|$ and $|y|$ are the distances between the field points along axes x and y.

The homogeneous and anisotropic function (3.9) takes into account the relationship between the field points in a certain limited area defined by the damping parameters. Due to the lack of comprehensive measurement data on the extent and distribution of corrosion zones, the parameters d_x and d_y of the correlation function (3.9) were adopted a priori $d = d_x = d_y = 0.05\ \mathrm{m}^{-1}$. The range of correlation is therefore relatively large. The calculations assume that the damping parameter d is a deterministic value.

The parameters of the correlation matrix have been selected so that the distribution of shell thickness variability t at a single point defines a normal distribution $N_t(\bar{t}, \sigma_t) \equiv N_t(24.7, 1.1)$ [mm]. 2000 realizations of the vessel corrosion fields were generated. The values of the expected critical force $\hat{P}_{\text{cr}}$ and its standard deviation $\hat{\sigma}_{P_{\text{cr}}}$ were estimated using PEM. For this purpose, the generated fields were classified according to the average value of the thickness t_{mean} of a single realization of the field. On this basis, the mean value $\hat{t}_{\text{mean}} = 24.69$ mm and standard deviation $\hat{\sigma}_{t_{\text{mean}}} = 1.095$ mm were determined. The histogram of the variable t_{mean} is shown in Fig. 8.

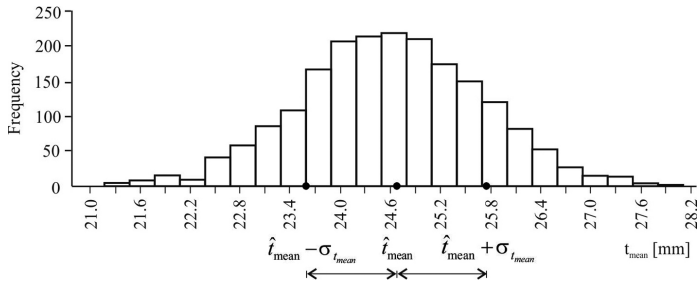

Fig. 8. Histogram of mean values t_{mean} of random fields of tank thickness

According to PEM, calculations should be made for two fields selected from 2000 generated realizations, defined by average shell thicknesses $t^{-}_{\text{mean}} = \hat{t}_{\text{mean}} - \hat{\sigma}_{t_{\text{mean}}}$ and $t^{+}_{\text{mean}} = \hat{t}_{\text{mean}} + \hat{\sigma}_{t_{\text{mean}}}$. An example of a corrosion field is shown in Fig. 9a.

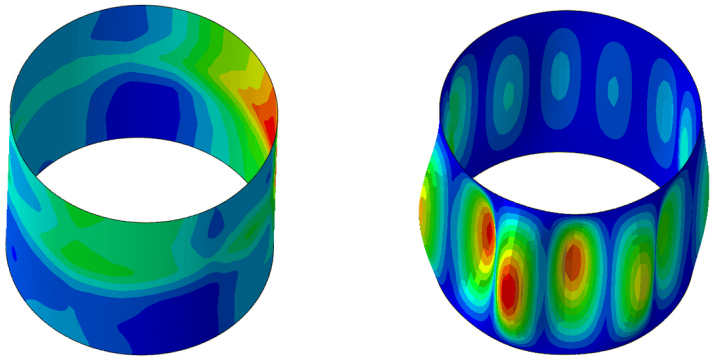

(a) (b)

Fig. 9. Corrosion described by a random field ($t^{-}_{\text{mean}} = \hat{t}_{\text{mean}} - \hat{\sigma}_{t_{\text{mean}}}$): (a) corrosion distribution; b) critical shell deformation

For the selected two implementations of the medium thickness field t_{mean}, FEM calculations were performed, obtaining the following results:

$$\begin{aligned} t^{-}_{\text{mean}} &= 24.7 - 1.095 = 23.602 \text{ mm} \quad \rightarrow \quad \text{P}^{-}_{\text{cr}} = -0.7427 \text{ MPa} \\ t^{+}_{\text{mean}} &= 24.7 + 1.095 = 25.792 \text{ mm} \quad \rightarrow \quad \text{P}^{+}_{\text{cr}} = -0.9653 \text{ MPa} \end{aligned} \tag{3.10}$$

Based on these calculations, using the PEM formulas (3.1), the estimators of the average critical force $\hat{P}_{\text{cr}} \approx -0.854$ MPa, and standard deviation $\hat{\sigma}_{P_{\text{cr}}} = 0.1113$ MPa were determined. The deformation of the tank model is presented in Fig. 9b.

4. Summary and conclusion

The results of all calculations are presented in Tab. 1. The mean values $\hat{P}_{\text{cr}}$ of the four critical forces differ slightly, but the methods of describing the corrosion distributions affect the values of the standard deviations $\hat{\sigma}_{P_{\text{cr}}}$. Almost identical values $\hat{\sigma}_{P_{\text{cr}}}$ were obtained in three cases, i.e.: corrosion described by one variable – shell thickness t, two variables – sine functions and thickness$t$, and random field. Much lower values of the standard deviation $\hat{\sigma}_{P_{\text{cr}}}$ were obtained for the corrosion model defined by two random variables, i.e. the angle α and the shell thickness t. In this case, the deterioration of the shell covering is only a part of the tank. Other models describe changes in the thickness of the entire shell.

Table 1. Critical force values P_{cr} vs. tank corrosion models

	Uniform thickness t [MPa]	**Angle α and thickness t [MPa]**	**Sine functions and thickness t [MPa]**	**Random Field – thickness t [MPa]**
$\hat{P}_{\text{cr}}$	–0.872	–0.854	–0.869	–0.854
$\hat{\sigma}_{P_{\text{cr}}}$	0.102	0.050	0.102	0.111

In the random field model of tank corrosion, the value of the damping parameter d was arbitrarily adopted. Changing this value will change the calculation results. In this sense, corrosion described by a random field has the most general character. However, no parametric analysis of the influence of the damping parameter d on the estimation of the expected value $\hat{P}_{\text{cr}}$ and standard deviation $\hat{\sigma}_{P_{\text{cr}}}$ was performed. Such calculations could also indicate the most unfavorable range of correlations due to the load capacity of the structure.

In addition, the sensitivity of the critical force P_{cr} value to a change in the shell corrosion model was checked. Figure 10 shows the values of critical forces determined for the mean values of random variables describing corrosion m_y, and for the mean values reduced and increased by their standard deviation σ_y i.e. $m_y \mp \sigma_y$, where the variable y describes the corrosion model parameters. In three cases, i.e. corrosion zones described by a uniform change in thickness $y \equiv t$, a sine function change $y \equiv n_y$, and a random field $y \equiv t_{\text{mean}}$, the obtained critical forces do not differ much. In addition, in these cases, linear relationships between the obtained results can be found. Only the values obtained for the corrosion field described by the angle $\alpha(y \equiv \alpha)$ deviate from these solutions (Fig. 10).

An important element of the analysis was to determine which of the corrosion models can be considered useful in the design process and engineering calculations. Degradation of the shell thickness described by one variable – the thickness t is the easiest to use, but this type of corrosion model is not confirmed by measurements of real objects. However, comparing the obtained solutions with other corrosion models (Table 1 and Fig. 10), it can be concluded

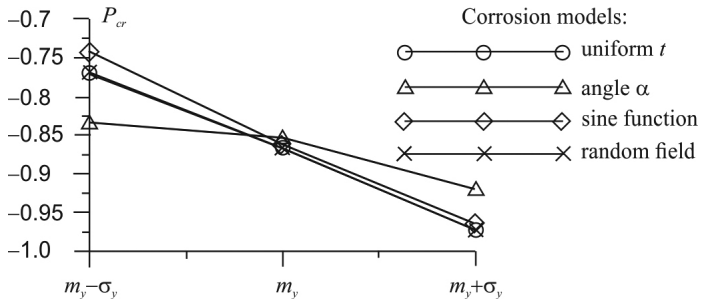

Fig. 10. The sensitivity of the shell critical force P_{cr} to a change in the corrosion model

that this type of simplified analysis well reflects the critical states of the tank. Thus, in the absence of comprehensive measurement data, a homogeneous corrosion model described by one variable – shell thickness t – is the best solution. Moreover, following the standards [3], protection against loss of load capacity of horizontal pressure tanks consists of introducing a corrosion additive, i.e. increasing the thickness of the shell. The standard guidelines therefore correspond to the simplest corrosion model.

The calculations focused only on the impact of vessel corrosion, ignoring other factors such as geometric imperfections or external factors, i.e. nonuniform settlement or seismic load. Estimated expected values $\hat{P}_{\mathrm{cr}}$ and standard deviations $\hat{\sigma}_{P_{\mathrm{cr}}}$ are therefore not objective parameters determining the actual load capacity of pressure vessels. The proposed corrosion models can also be used in the analysis of other structures, e.g. vertical tanks, silos, as well as shipbuilding.

Acknowledgements

The authors acknowledge the access to computational software provided by the Centre of Informatics – Tricity Academic Supercomputer & network (CI TASK) and the financial support by the Innovative Economy Operational Programme [POIG.01.04.00-24-073/09-03].

References

[1] Directive 2014/68/EU of the European Parliament and of the Council of 15 May 2014 on the harmonisation of the laws of the Member States relating to the making available on the market of pressure equipment.

[2] EN 1990 Eurocode – Fundamentals of structural design.

[3] EN 1993-6 Eurocode 3 – Design of steel structures part 4–2. Tanks.

[4] A. Niloufari, H. Showkati, M. Maali, and S.M. Fatemi, "Experimental investigation on the effect of geometric imperfections on the buckling and post-buckling behavior of steel tanks under hydrostatic pressure", *Thin-Walled Structures*, vol. 74, pp. 59–69, 2014, doi: 10.1016/j.tws.2013.09.005.

[5] K. Rasiulis, A. Šapalas, R. Vadlūga, and M. Samofalov, "Stress/strain state investigations for extreme points of thin wall cylindrical tanks", *Journal of Constructional Steel Research*, vol. 62, no. 12, pp. 1232–1237, 2006, doi: 10.1016/j.jcsr.2006.04.016.

[6] R. Ignatowicz and E. Hotala, "Failure of cylindrical steel storage tank due to foundation settlements", *Engineering Failure Analysis*, vol. 115, pp. 1–8, 2020, doi: 10.1016/j.engfailanal.2020.104628.

[7] J.I. Colombo, R.A. Herrera, and J.L. Almazán, "Low cycle fatigue capacity of shell-to-base connections in stainless steel thin-walled tanks", *Engineering Structures*, vol. 245, 2021, doi: 10.1016/j.engstruct.2021.112949.

[8] P.K. Malhotra, P. Nimse, and M. Meekins, "Seismic sloshing in a horizontal liquid storage tank", *Structural Engineering International*, vol. 24, no. 4, pp. 466–473, 2014, doi: 10.2749/101686614X13854694314928.

[9] P.G. Cirimello, J.L. Otegui, D. Ramajo, and G. Carfi, "A major leak in a crude oil tank: Predictable and unexpected root causes", *Engineering Failure Analysis*, vol. 100, pp. 456–469, 2019, doi: 10.1016/j.engfailanal.2019.02.005.

[10] W. Geary and J. Hobbs, "Catastrophic failure of a carbon steel storage tank due to internal corrosion", *Case Studies in Engineering Failure Analysis*, vol. 1, no. 4, pp. 257–264, 2013, doi: 10.1016/j.csefa.2013.09.002.

[11] A. Rahbar-Ranji, "Ultimate strength of corroded steel plates with irregular surfaces under in-plane compression", *Ocean Engineering*, vol. 54, pp. 261–269, 2012, doi: 10.1016/j.oceaneng.2012.07.030

[12] E. Gutman, J. Haddad, and R. Bergman, "Stability of thin-walled high-pressure vessels subjected to uniform corrosion", *Thin-Walled Structures*, vol. 38, no. 1, pp. 43–52, 2000, doi: 10.1016/S0263-8231(00)00024-0.

[13] M.M. Hossain and R. Seshadri, "Simplified fitness-for-service assessment of pressure vessels and piping systems containing thermal hot spots and corrosion damage", *International Journal of Pressure Vessels and Piping*, vol. 87, no. 7, 2010, doi: 10.1016/j.ijpvp.2010.04.001.

[14] P. Tantichattanont, S.M.R. Adluri, and R. Seshadri, "Structural integrity evaluation for corrosion in spherical pressure vessels", *International Journal of Pressure Vessels and Piping*, vol. 84, no. 12, pp. 749–761, 2007, doi: 10.1016/j.ijpvp.2006.12.004.

[15] M. Cerit, "Corrosion pit-induced stress concentration in spherical pressure vessel", *Thin-Walled Structures*, vol. 136, pp. 106–112, 2019, doi: 10.1016/j.tws.2018.12.014.

[16] Y. Pronina, O. Sedova, M. Grekov, and T. Sergeeva, "On corrosion of a thin-walled spherical vessel under pressure", *International Journal of Engineering Science*, vol. 130, pp. 115–128, 2018, doi: 10.1016/j.ijengsci.2018.05.004.

[17] O. Sedova and Y. Pronina, "The thermoelasticity problem for pressure vessels with protective coatings, operating under conditions of mechanochemical corrosion", *International Journal of Engineering Science*, vol. 170, 2022, doi: 10.1016/j.ijengsci.2021.103589.

[18] Y. Choi, J. Ahn, and D. Chang, "Time-dependent reliability analysis of plate-stiffened. Prismatic pressure vessel with corrosion", *Mathematics*, vol. 9, no. 13, art. no. 1544, 2021, doi: 10.3390/math9131544.

[19] N. Habibi, S. Mohammadi, and H. Ghafary, "Reliability of steel cylindrical pressure vessel dividers in the presence of corrosion. experiment and simulation", *International Journal of Steel Structures*, vol. 23, no. 2, pp. 599–612, 2023, doi: 10.1007/s13296-023-00715-5.

[20] N. Kasai, T. Maeda, K. Tamura, S. Kitsukawa, and K. Sekine, "Application of risk curve for statistical analysis of backside corrosion in the bottom floors of oil storage tanks", *International Journal of Pressure Vessels and Piping*, vol. 141, pp. 19–25, 2016, doi: 10.1016/j.ijpvp.2016.03.014.

[21] K. Woloszyk and Y. Garbatov, "Advanced numerical modelling for predicting residual compressive strength of corroded stiffened plates", *Thin-Walled Structures*, vol. 183, 2023, doi: 10.1016/j.tws.2022.110380.

[22] M. Maslak and M. Pazdanowski, "Time-to-failure forecast for corroded shell of above-ground steel tank used to store liquid fuels", *Archives of Civil Engineering*, vol. 67, no. 1, pp. 303–322, 2021, doi: 10.24425/ace.2021.136475.

[23] M. Kamiński and P. Świta, "Structural stability and reliability of the underground steel tanks with the Stochastic Finite Element Method", *Archives of Civil and Mechanical Engineering*, vol. 15, pp. 593–602, 2015, doi: 10.1016/j.acme.2014.04.010.

[24] K. Kubicka and U. Radon, "The system reliability of steel trusses with correlated variables", *Archives of Civil Engineering*, vol. 70, no. 2, pp. 163–178, 2024, doi: 10.24425/ace.2024.149857.

[25] P. Zabojszcza, U. Radon, and P. Tauzowski, "Robust and reliability-based design optimization of steel beams" *Archives of Civil Engineering*, vol. 69, no. 4, pp. 125–140, 2023, doi: 10.24425/ace.2023.147651.

[26] E. Rosenblueth, "Point estimates for probability moments", *Proceedings of the National Academy of Sciences of U.S.A.*, vol. 72, no. 10, 1975, doi: 10.1073/pnas.72.10.3812.

[27] R.E. Melchers and A.T. Beck, *Structural reliability analysis and prediction*. John Wiley & Sons Ltd., 2018, doi: 10.1002/9781119266105.

[28] P.H. Waartsa and A.C.W.M. Vrouwenveldera, "Stochastic finite element analysis of steel structures", *Journal of Constructional Steel Research*, vol. 52, pp. 21–32, 1999.

[29] P. Sorn, M. Sondej, and J. Górski, "Reliability estimation of underground fuel tank", *Bulletin of the Polish Academy of Sciences. Technical Sciences*, vol. 71, no. 2, 2023, doi: 10.24425/bpasts.2023.144588.

[30] M. Smith, *ABAQUS/Standard User's Manual, Version 6.9*. Providence, RI: Dassault Systèmes Simulia Corp, 2009.

[31] E. Korol, "SFEM Analysis of Beams with Scaled Lengths including Spatially Varying and Cross- Correlated Concrete Properties", *Materials*, vol. 15, no. 1, 2022, doi: 10.3390/ma15010095.

[32] H. Walukiewicz, E. Bielewicz, and J. Górski, "Simulation of nonhomogeneous random fields for structural applications", *Computers and Structures*, vol. 64, no. 1–4, pp. 491–498, 1997.

[33] E. Bielewicz and J. Górski, "Shells with random geometric imperfections simulation - Based approach", *International Journal of Non-Linear Mechanics,* vol. 37, no. 4–5, pp. 777–784, 2002, doi: 10.1016/S0020-7462(01)00098-1.

[34] J. Górski, T. Mikulski, M. Oziębło, and K. Winkelmann, "Effect of geometric imperfections on aluminium silo capacities", *Stahlbau*, vol. 84, 2015, doi: 10.1002/stab.201510224.

[35] K. Winkelmann and J. Górski, "The use of Response Surface Methodology for reliability estimation of composite engineering structures", *Journal of Theoretical and Applied Mechanics*, vol. 52, no. 4, pp. 1019–1032, 2014.

Probabilistyczne modele korozji podziemnego poziomego zbiornika ciśnieniowego

Słowa kluczowe: podziemne zbiorniki ciśnieniowe, korozja powłok, stany graniczne, opis probabilistyczny

Streszczenie:

Awaria zbiorników ciśnieniowych na paliwa i inne materiały petrochemiczne może doprowadzić do skażenia środowiska, a także zagrażać zdrowiu i życiu ludzi. Wytyczne normowe wymagają aby niezawodność zbiorników w przewidzianym okresie eksploatacji była odpowiednio wysoka. Określa się ją na podstawie ściśle zdefiniowanej miary – wskaźnika niezawodności β. Jednocześnie przyjmuje się, że odpowiedni poziom niezawodności zbiorników uzyska się stosując wskazane w normach algorytmy obliczeniowe. Tylko w przypadku klasy konsekwencji CC3 konstrukcji konieczne jest liczbowe oszacowanie wskaźnika niezawodności β. W normach jednak nie wskazano w jaki sposób takie obliczenia powinny być wykonywane. Wydaje się istotne wypełnienie wyraźnej luki pomiędzy normowymi wytycznymi a powszechnie stosowanymi metodami projektowania. Analiza zbiorników powinna dotyczyć wielu niestandardowych elementów jak np. imperfekcji geometrycznych i materiałowych, nierównomiernego osiadani czy procesów korozyjnych. W pracy wykonano analizę probabilistyczną skorodowanego zakopcowanego poziomego zbiornika ciśnieniowego na paliwa płynne. Rozpatrzono kilka wariantów opisu korozji: jednorodną zmianę grubości blachy powłoki, zmniejszenie grubości fragmentu walca określonego kątem α, wprowadzenie regularnych obszarów korozji opisanych funkcją sinus oraz symulację stref korozji polami losowymi. Celem pracy było sprawdzenie jak poszczególne modele korozji wpływają na zmianę siły krytycznej niszczącej powłokę w wyniku działania podciśnienia. Obliczenia MES wykonano dla fragmentu zbiornika (walca) z warunkami brzegowymi modelującymi żebra usztywniające. Z uwagi na specyfikę obciążenia zbiornika podciśnieniem nie ma potrzeby analizy całej konstrukcji. Zastosowano analizę probabilistyczną. Grubość t powłoki zdefiniowano za pomocą rozkładu Gaussa o średniej równej grubości powłoki pomniejszonej o naddatek korozyjny. Odchylenie standardowe zmiennej t przyjęto w taki sposób aby maksymalna grubość powłoki nie przekraczała jej rzeczywistej grubości. Kąt α opisujący fragmentaryczną korozję walca opisano rozkładem równomiernym. W podobny sposób przyjęto liczbę fal w sinusoidalnym opisie uszkodzenia powłoki. Opis korozji za pomocą pól

losowych najlepiej odwzorowuje rzeczywisty charakter zniszczenia powłoki. Dobrano odpowiednią funkcję korelacyjną umożliwiającą symulację nieregularnych obszarów korozji. Celem obliczeń losowych jest uzyskanie informacji o rozrzutach siły krytycznej powłoki. W pracy zastosowano algorytm obliczeń wykorzystujący Metodę Estymacji Punktowej (PEM). Zgodnie z tą metodą w przypadku jednej zmiennej należy wykonać jedynie dwa obliczenia dla wartości oczekiwanej pomniejszonej i powiększonej o jej odchylenie standardowe. Wariant dwóch zmiennych wymaga wykonanie odpowiedniej analizy czterech przypadków. Metodę PEM zastosowano konsekwentnie we wszystkich czterech wariantach opisu korozji. W przypadku ciągłych zmiennych losowych, a więc zmiany grubości powłoki t i kąta wypełnienia α analiza probabilistyczna ma standardowy charakter. Natomiast w wariancie opisu zakresu korozji za pomocą liczby fal funkcji sinus obliczenia mają charakter przybliżony. Z kolei definicja pól losowych wymagała przeprowadzenie ich klasyfikacji zgodnie z wartością średnią grubości powłoki pojedynczej realizacji i na tej podstawie wyznaczenia globalnego odchylenie standardowego. Wykonane obliczenia wykazały, że dla trzech wariantów opisu korozji, tj. równomiernej zmiany grubości t, zmiennej grubości zdefiniowanej funkcją sinus oraz korozji opisanej polami losowymi otrzymano niemalże identyczna wartości siłkrytycznych i jej odchylenia standardowego. Tylko w przypadku modelu definiującego zakres korozji za pomocą kąta α wartość oczekiwana jest nieznacznie mniejsza. Ponadto analiza wrażliwości zmiany siły krytycznej na zmianę parametrów korozyjnych w trzech pierwszych przypadkach wykazała ich liniowy charakter. Nieliniową zmianę uzyskano jedynie dla opisu korozji za pomocą kątem α. Odpowiednie obliczenia wykonano zmniejszając i zwiększając wartości zmiennych losowych o ich odchylenia standardowe. Przeprowadzona analiza pozwala na sformułowanie wniosków dotyczących modelowania korozji. W przypadku obliczeń inżynierskich wydaje się właściwe przyjęcie najprostszego modelu, tj. jednorodnej zmiany grubości powłoki. Znacznie bardziej skomplikowane obliczenia przy wykorzystaniu np. pól losowych nie wpływają na zmianę wyników. Ponadto taki uproszczony model jest zgodny z normowymi wytycznymi związanymi z powiększaniem grubości powłoki o tzw. naddatek korozyjny. Uzyskane rozwiązania pozwalają na wyznaczenie możliwych rozrzutów siły krytycznej a w konsekwencji do oszacowania zmniejszanie niezawodności zbiornika w miarę upływu czasu jego eksploatacji. Należy podkreślić, że w przypadku uzyskania danych dotyczących rzeczywistego zakresu korozji zbiornika można wykonać udokładnione obliczenia. Dotyczy to przede wszystkim modelu korozji opisanej polem losowym. Rzeczywiste dane z oględzin skorodowanego zbiornika pozwolą na dobranie odpowiedniej długości korelacyjnej. To same wnioski można sformułować w przypadku korozji opisanej kątem α. Praca wskazuje także na zalety stosowania metody PEM pozwalającej na szybkie i łatwe oszacowanie wartości oczekiwanej i odchylenia standardowego siły krytycznej. Zaproponowany algorytm uwzględniający wpływ korozji w obliczeniach obciążeń krytycznych zbiorników ciśnieniowych można bezpośrednio zastosować w analizie innych zbiorników, silosów lub generalnie konstrukcji powierzchniowych.

Received: 2024-06-23, Revised: 2024-09-10